JOURNAL OF MATERIALS SCIENCE 12 (1977) 1625–1638

Prediction of the yielding behaviour of rolled polyoxymethylene

N. D. CRISP, M. J. MILES,* N. J. MILLS
Department of Physical Metallurgy and Science of Materials, University of Birmingham, Birmingham, UK

The yield stress anisotropy of rolled polyoxymethylene (a semicrystalline polymer) is predicted by treating the polymer as a polycrystalline aggregate having two types of crystal slip system. The model first predicts the texture development on cold rolling, then the angular variation in yield stress for various uniaxial stress and plane strain compression tests. At present the model has four disposable parameters (the critical resolved shear stresses for chain and prism slip, a strain hardening coefficient and a minimum yield stress on reverse yielding), which are amenable to experimental confirmation.

1. Introduction

Previous attempts to describe the yielding behaviour of anisotropic polymers have been of two main kinds. Firstly Hill's yield criterion for an anisotropic material with three mutually perpendicular planes of symmetry [1] has been used in a modified form [2] that includes a Bauschinger effect. Secondly a single crystal plasticity approach has been used for highly oriented polyethylene [3] and polypropylene [4], assuming that various deformation mechanisms can occur with different critical resolved shear stresses. Neither approach is ideal; the modified Hill's yield criterion contains a number of constants with no clear physical significance, and the single crystal plasticity approach neglects the distribution of crystal orientations (texture) that exists in most anisotropic polymers. We have previously [5]† proposed a model for the development of texture in polyoxymethylene (POM) when sheets of the material are cold rolled. In this paper that approach is extended to the prediction of the yielding behaviour. It is an approach using several deformation mechanisms in each "crystal", but also considering the spread of crystal orientations in a polycrystalline aggregate. The texture prediction [5] is now briefly reviewed and improvements described before discussing the application of the approach to yield anisotropy prediction.

2. Theory

2.1. Crystal–slip model for the prediction of texture development in POM on rolling

In the polycrystalline model the amorphous interlamellar material is incorporated into a redefined "crystal" shown in Fig. 1. These *crystals* are assumed to be randomly oriented in the undeformed POM, and have the following three deformation mechanisms.

(a) $\{1\,0\,\bar{1}\,0\}$ [0 0 0 1] slip in the lamellar crystals–chain slip. This is slip on the growth (fold) planes found in single crystals of POM, in the chain axis direction.

(b) $\{1\,0\,\bar{1}\,0\}$ $\langle 1\,\bar{2}\,1\,0\rangle$ slip in the lamellar crystals–prism slip.

(c) Elastic interlamellar shear in the amorphous phase. This mechanism is required to achieve

*Present address: Universität des Saarlandes, Werkstoffphysik, 66 Saarbrucken, Germany

†*Erratum in reference [5] page 2102*
The formula for the 0 0 0 1 pole figure intensity of the Wilshinsky model should read

$$I = r^3/(\cos^2\beta^1 + wr^2\sin^2\beta^1)^{3/2}$$

This change makes no noticeable change in the predicted pole figures.

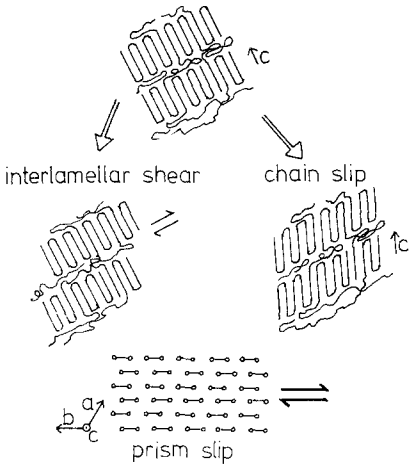

Figure 1 The *crystal* in POM and its deformation mechanisms.

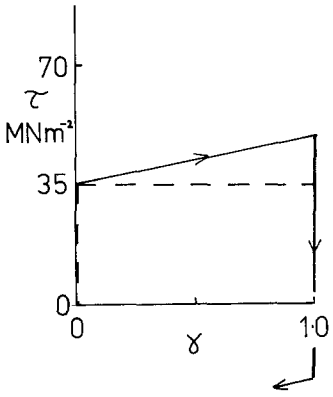

Figure 2 Shear stress–strain relationship postulated for the chain slip process. SHC = 0, – – – –, SHC = 0.4 ———.

extension parallel to the c axis of the *crystal,* but it is assumed to be limited in amount and reversible, so that it does not directly lead to texture development, or initiate yielding.

No account is taken of any long range interactions between *crystals* such as might occur in a spherulite, or of any microvoiding that is known to occur in the tensile deformation of POM.

Unidirectional rolling is approximately a plane strain deformation process in the RN plane (R rolling direction, T transverse direction, N sheet normal) because the plastic strain in the transverse direction is very small. If r is the ratio of the final to the initial sheet thickness, then the true strain in the N direction $\epsilon_N = \ln r$, and the true strain in the rolling direction $\epsilon_R = -\ln r$. Previously [5] the polymer was assumed to obey the Von Mises yield criterion at all stages of rolling. Experimental evidence, to be presented later in this paper, shows that this is not the case once the POM becomes anisotropic. Therefore the stress tensor with respect to the axes RTN in the sheet is assumed to be

$$\begin{pmatrix} 0 & 0 & 0 \\ 0 & -qk_i & 0 \\ 0 & 0 & -2k_i \end{pmatrix}$$

q is taken to be 1 initially to correspond to a Von Mises yield criterion, but its value is adjusted as rolling proceeds so that the average plastic strain in the T direction remains zero. k_i is adjusted so that the critical resolved shear stress of the most favoured of the 6 crystal slip systems is just reached in the ith crystal. The macroscopic, or average, stress tensor in the roll nip is assumed to be of the above form, but with $\bar{k}$ replacing k_i where

$$\bar{k} = n \Big/ \sum_{i=1}^{n} (1/k_i) \qquad (1)$$

Note that the assumptions about the stresses in the polycrystal, and that single slip occurs in each *crystal,* means that there will not be displacement continuity at the *crystal* boundaries.

A second refinement was to introduce strain hardening into the assumed stress–strain relation for chain slip in the *crystal.* The reason for doing this was that the predicted increase in $\bar{k}$ as rolling proceeded and crystal orientation developed (orientation hardening) was less than the observed effect [5]. Therefore it was proposed that the critical resolved shear stress for each chain slip system increased proportionately to the shear strain on that system (Fig. 2), but that there was no hardening for prism slip. The justification for this assumption was that chain slip and interlamellar shear are likely to be linked, (Fig. 1) and that the rubber elasticity hardening of the latter would hinder the former. It was found that an increase of 40% in critical resolved shear stress per unit shear strain, for a critical resolved shear stress ratio of 2.5:1 (prism:chain), produced the best correspondence in Fig. 3.

Once the active slip system had been established for each *crystal,* it was assumed that a shear strain of 0.1 occurs on that system. From this strain increment the *crystal* reorientation was found using the two constraints that, before and after shear in the crystal (i) material lines parallel to the R direction, and (ii) material planes parallel to the

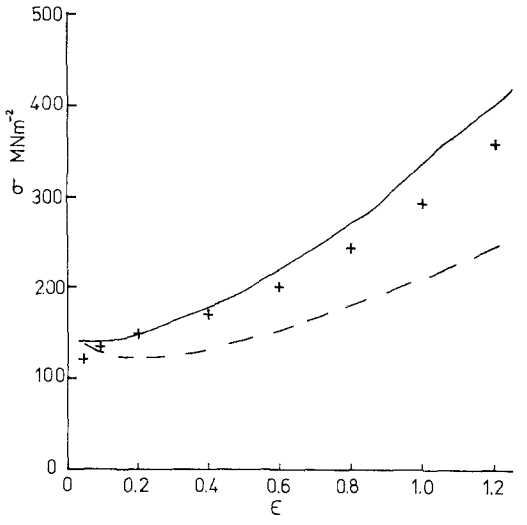

Figure 3 True stress–true strain relationship for the plane strain compression of initially isotropic POM. Prediction for CHAIN = 35 MN m^{-2}, PRISM = 87.5 MN m^{-2} and SHC = 0 – – – –; Prediction for SHC = 0.4 ———. Experimental values of the plastic strain after loading from the maximum stresses shown +.

RT plane maintain their orientation. Once the new orientations were found, the process of finding the active slip system in each *crystal* could be started again, and continued until the macroscopic average strains reached the required level.

A third refinement was to treat the orientation distribution of the polycrystalline model, in a similar way to that used for experimental polefigure data, to produce contour levels on 0 0 0 1, 1 0 $\bar{1}$ 0 and 1 0 $\bar{1}$ 5 polefigures, rather than showing individual pole positions as in [5]. This makes comparisons with experimental polefigures easier. A 10 x 10 square grid was superimposed on the stereographic projection of one quadrant of the relevant polefigure and the number of poles falling in each grid square counted. This number was compared with the number that would fall in the same square from a random orientation distribution, the contour levels of 0.4, 1, 2, 4, times random intensity calculated. Note that the 0 0 0 1 X-ray diffraction peak from a POM crystal is that from planes separated by the *c* dimension of the unit cell, 1.74 nm. This diffraction peak is not observed experimentally, but the 0 0 0 9 peak (from planes separated by *c*/9) is observed and this gives equivalent information. However the 0 0 0 9 diffraction peak is not easily resolved from the stronger 1 1 $\bar{2}$ 5 peak, which makes it almost impossible to obtain the information for a 0 0 0 1 pole figure of POM. In polytetrafluoroethylene (PTFE), which also has a hexagonal unit cell (if the spiral form of each chain is ignored), the 0 0 0 1 5 diffraction peak is readily observed, so we have used the pole figure from this as a partial substitute for the unavailable POM 0 0 0 1 pole figure.

The effects of maintaining a plane strain deformation in rolling, and of introducing strain hardening, on the texture predictions of the model were minor. However having the predictions in the form of contour "maps" permitted a more critical comparison with the experimental data in [5]. The resulting conclusions are

(i) The effect of increasing the ratio of the critical resolved shear stress for prism slip to that for chain slip is to reduce the proportion of crystals whose orientation can be described approximately as $\{1\,\bar{2}\,1\,0\}\ \langle 1\,0\,\bar{1}\,0\rangle$ i.e. with a 1 $\bar{2}$ 1 0 plane parallel to the RT plane and a 1 0 $\bar{1}$ 0 direction along R. If this ratio is 2.5:1 the predictions are close to the experimental data at a true strain $\epsilon_R = 0.69$, but a higher ratio of about 8:1 is required at $\epsilon_R = 1.20$.

(ii) The texture is predicted to develop more rapidly with rolling reduction than occurs in practise. Fig. 4 shows that the predictions for $\epsilon_R = 0.36$ roughly match the textures observed at $\epsilon_R = 0.69$, and Fig. 5 shows that the predictions at $\epsilon_R = 0.69$ roughly match the observed texture at $\epsilon_R = 1.20$. Fig. 4 includes a 0 0 0 1 5 polefigure for PTFE that has been plane strain compressed at 18° C to $\epsilon_R = 0.76$. The 1 0 $\bar{1}$ 0 polefigure for this material is very similar to that shown for POM, so it is assumed that it has a similar texture to the POM.

(iii) The one element of the predicted texture that is not observed is that described as: 0 0 0 1 axis approaching a position 40° from R in the RT plane. It is caused by the 0 0 0 1 axis of a crystal getting to within roughly 20° of R by chain slip, wherupon prism slip is then reactivated and rotation towards the final position occurs by a mixture of chain and prism slip. Further changes were then made in the texture prediction programme to obtain the polefigure predictions shown on the bottom rows of Figs. 4 and 5. These changes were (a) Crystals with 0 0 0 1 axes that had rotated to within about 20° of R were assumed to continue to rotate as if chain slip had occurred, even if prism slip had occurred. (b) Once the required thickness reduction was achieved, the

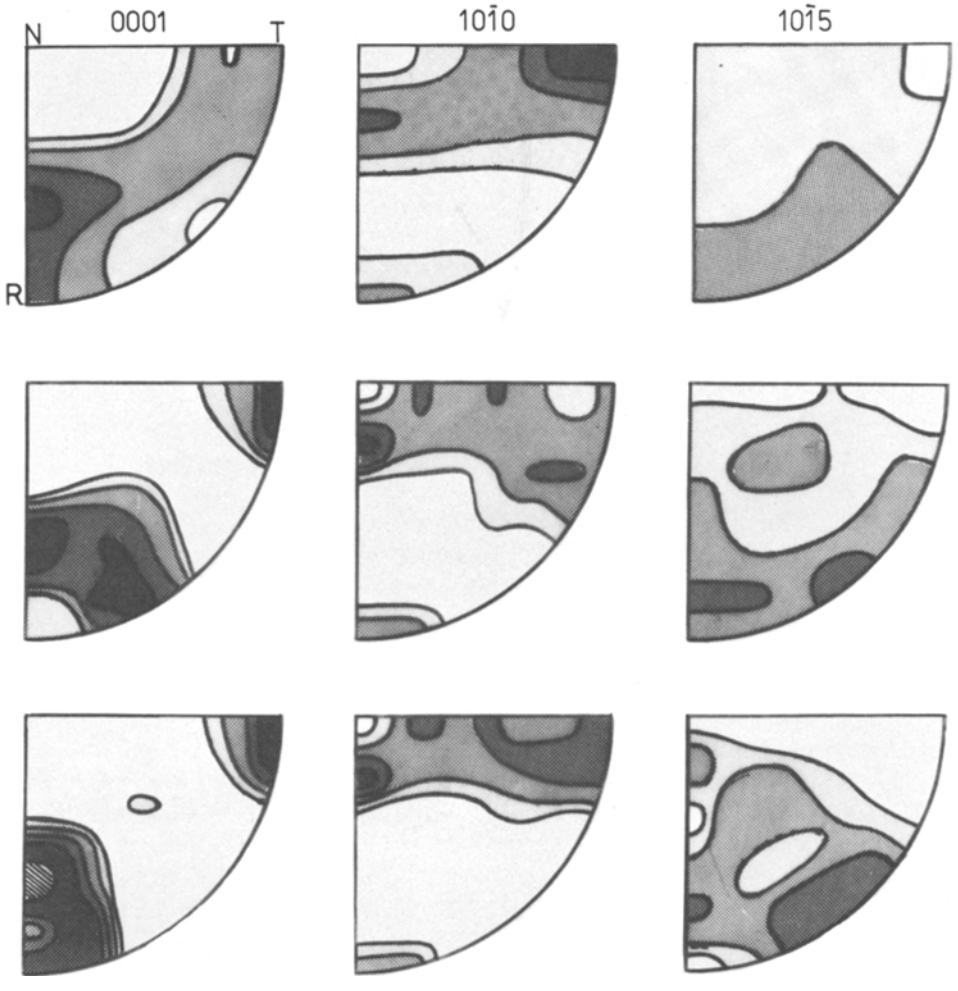

Figure 4 Polefigures for uniaxially rolled POM. Top row experimental at $\epsilon_R = 0.69$ (0 0 0 1 polefigure is for PTFE). Middle row are predictions at $\epsilon_R = 0.36$ for PRISM/CHAIN = 2.5 and with no restrictions on rotation due to prism slip. Bottom row are predictions at $\epsilon_R = 0.36$ for PRISM/CHAIN = 2.5, with the modifcations (a) and (b) of Section 2.

Euler angles α of all crystals with $|\alpha| > 40°$ were increased so that the difference between $|\alpha|$ and 90° was halved.

The effect was to concentrate the main intensity peak in the 0 0 0 1 polefigure toward the RN plane, and to improve the correspondence of the 1 0 $\bar{1}$ 0 and 1 0 $\bar{1}$ 5 polefigures with experimental ones.

Although it is possible to reproduce the main features of the observed polefigures using a simple model, it is very difficult to predict the exact texture. The major problem seems to be in the constraints used to predict crystal rotation. Those used are separately valid for tensile and compressive tests on single crystals of certain shapes, but their use in combination for the plane strain deformation of crystals of unknown shape in a polycrystalline aggregate has never been justified theoretically. The changes made in (iii) above to get a better correspondence with experiment reinforce this point.

It was decided to use the textures shown on the bottom rows of Figs. 4 and 5 as a close approximation to the experimental textures.

2.2. Prediction of yield stress anisotropy

Predictions were only made for tests for which experimental data had been gathered. These were firstly uniaxial tension and uniaxial compression tests, and secondly two types of plane strain compression test. Some caution must be exercized in the use of terms uniaxial tension test, etc; al-

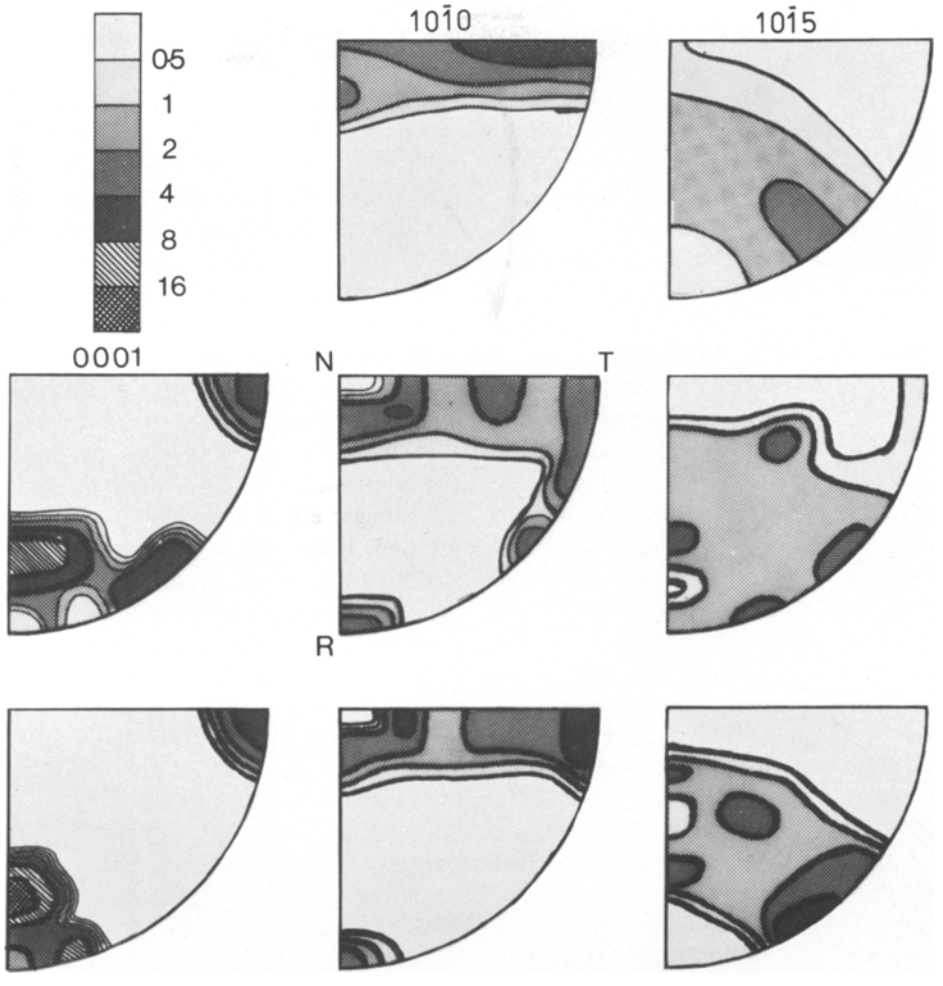

Figure 5 As Fig. 4 except that the experimental data is for $\epsilon_{\mathbf{R}} = 1.20$, and the predictions are for $\epsilon_{\mathbf{R}} = 0.69$.

though the applied stress is a uniaxial tensile stress, the resulting strains in an anisotropic material may well be more complex, i.e. there may be shear strains as well as tensile components of strain. This will not matter in the uniaxial stress tests for we allow other shear strains to occur at will, in calculating the yield stress. Even in the plane strain compression calculations, where the three tensile components of strain with respect to the testing device axes are specified, there is no restriction on a shear strain occurring in the plane of plastic deformation. As long as the plane of plastic deformation is a symmetry plane of the material, such as the RT plane, the material should deform as required under the imposed stresses.

Uniaxial compression tests (carried out as in [4]), Ford plane strain compression tests [6], and plane strain compression tests in a slot [7] were carried out in axes R′T′N which are related to the sheet axes RTN by a rotation of θ about the N axis. The applied stress tensors in the three tests are assumed to be of the forms

$$\begin{pmatrix} -2k & 0 & 0 \\ 0 & 0 & 0 \\ 0 & 0 & 0 \end{pmatrix}, \quad \begin{pmatrix} 0 & 0 & 0 \\ 0 & -qk & 0 \\ 0 & 0 & -2k \end{pmatrix},$$

$$\begin{pmatrix} 0 & 0 & 0 \\ 0 & -2k & 0 \\ 0 & 0 & -qk \end{pmatrix}$$

respectively in the R′T′N axes. The plane of plastic deformation in the plane strain compression tests is R′N for the Ford test (Fig. 6) and R′T′ for the slot test (Fig. 7). From the discussion above, the stresses in the Ford test should also include the

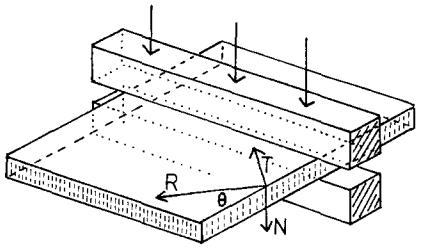

Figure 6 Apparatus for the Ford plane strain compression test in the R'N plane.

shear stresses necessary to maintain $e_{R'T} = e_{NT'} = 0$, but in this analysis these shear stresses have been ignored. The slot test does not have this drawback if the plane of deformation is the R'T' ≡ RT plane. The slot test has a further advantage for investigating Bauschinger effects. Previous workers [2] used pure shear tests on waisted samples, but the elastic stress distribution in these prior to general yielding is complex. In the slot test the stress distribution should be homogeneous. Slot tests carried out for a particular value of θ can be compared with the same test carried out for $\theta' = 90 - \theta$, since in the θ' test the signs of the strain components e_{RR} and e_{TT} are reversed, whereas the shear strain e_{RT} is unchanged.

The stages in the calculation of the angular variation of the various yield stress determinations were as follows:

(1) An initial texture description (in terms of the Euler angles α, β, γ that relate the crystal axes of 187 crystals to the RTN axes) was chosen that was as close as possible to the experimental texture for POM rolled to a $\epsilon_R = 0.69$ or 1.20. This output from the texture prediction programme also included the cumulative shear strains on the six slip systems of each crystal.

(2) The stress tensor in the R'T'N axes of the yielding experiment was transformed into the RTN symmetry axes of the POM sheet, and then into the individual crystal axes. For each crystal the slip system with the highest ratio of resolved shear stress to critical resolved shear stress was determined. The critical resolved shear stress was assumed to depend on the previous strain history, as shown in Fig. 2. For the chain slip systems a linear strain hardening effect was assumed to occur, as explained earlier. Since it was postulated that this strain hardening is due to elastic strain in the interlamellar material, there should also be a Bauschinger effect when the direction of shear is reversed. If the interlamellar material aids reverse yielding to the same extent that it hinders forward yielding, then the change in shear stress to cause reverse yielding should be twice the original critical resolved shear stress (see Fig. 2). However there must be a limit to this process; if the interlamellar elastic stresses are large enough they should cause spontaneous reverse yielding when the crystal emerges from the roll nip. To model this limit for the polycrystalline aggregate it was assumed that the minimum resolved shear stress for reverse yielding was M times the original critical resolved shear stress (the magnitude of M was taken as a disposable parameter). In contrast with the chain slip process it was assumed that the prism slip process does not strain harden, and in consequence has no Bauschinger effect.

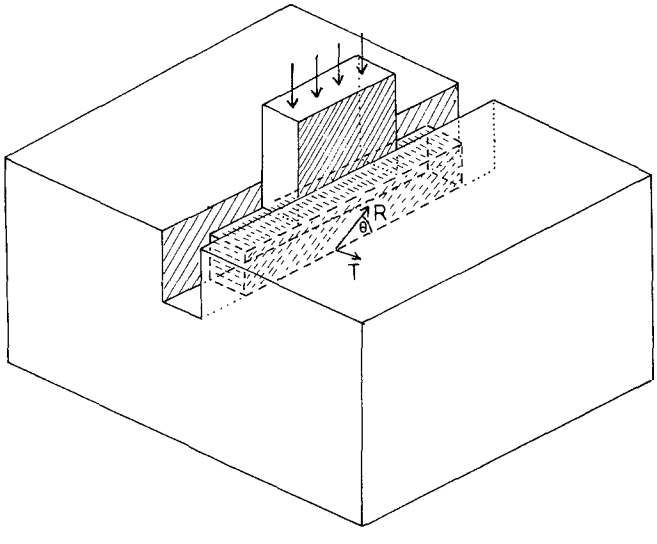

Figure 7 Apparatus for the slot plane strain compression test in the RT plane.

(3) For the plane strain compression experiments an estimate of the average plastic strains in the R′T′N axes was made. Each crystal was assumed to deform by single slip on the most favoured slip system, and an incremental shear strain of 0.1 was given to each crystal. Recalling that each crystal's axes are related to the R′T′N axes of the yielding test by the Euler angles $\alpha + \theta$, β, γ, the methods used in [5] were used to calculate L, the extension ratio of a material line initially along the most tensile principal stress axis, and r, the ratio of the final to initial separation of any two material planes that stay perpendicular to the most compressive principal stress axis. The average true strains in the R′ and T′ directions of the slot test, and the R′ and N directions of the Ford test, were calculated from the values of L and r. Finally, by assuming that plastic deformation occurs at constant volume, the true strain in the N direction of the slot test (T′ of Ford test) was calculated. If the magnitude of this strain exceeded 0.005, the value of q in the stress tensor was revised, and the calculation recommended from step 2.

(4) The values of the constants $\bar{k}$ in the stress tensor in the R′T′N axes were calculated as an average as the values k_i for individual crystals, using Equation 1.

(5) A correction was made for the known dependence [8, 9] of the yield stress of isotropic POM on the hydrostatic component σ_m of the applied stress. These workers found that the octahedral shear stress at yield τ_{oct} varied according to

$$\tau_{oct} = \tau_s - \mu\sigma_m$$

where the constant τ_s (= 50.3 MN m^{-2} at room temperature) is the pure shear yield stress for zero σ_m, and the constant μ was found to have the value 0.10. No similar measurements have been made on anisotropic POM, so it was assumed that the critical resolved shear stresses for chain and prism slip would change with σ_m in the same proportion as τ_{oct}. The uncorrected values of $\sigma_{R'R'}$ etc. (the components of the applied stress tensor in the R′T′N axes) were calculated in the previous step of the programme. From these we obtain the uncorrected value of σ_m

$$\sigma_{mu} = \tfrac{1}{3}(\sigma_{R'R'} + \sigma_{T'T'} + \sigma_{NN}).$$

The corrected values of the components of the stress tensor were then obtained by dividing the uncorrected components by the factor $(1 + \mu\sigma_{mu}/\tau_s)$.

Since some of the parameters of the model can be determined from experimental data, the predictions of the model will not be discussed until this data has been described. The computer programs are available from the authors on request.

3. Experimental determination of the yield stresses of POM

3.1. Material and apparatus

A high molecular weight polyoxymethylene copolymer (ICI Kematal 025) was compression moulded into sheets, and unidirectionally rolled at a low roll speed (about 35 mm sec^{-1}) and with reductions of about 0.2 mm per pass to a final thickness of 3 mm. The initial sheet thicknesses were such that the final thickness was either 0.5 or 0.3 of the initial thickness. The density of the POM was measured as 1.419 at 20° C, which indicates a volume fraction crystallinity of 0.74. For one set of experiments some commercially extruded POM copolymer sheet was unidirectionally rolled on a more powerful mill, (roll surface velocity 200 mm sec^{-1}, 0.3 mm reduction per pass) and in this case the temperature of the POM rose noticeably during rolling due to the rapid plastic deformation.

All the yield stress determinations were carried out on an Instron mechanical testing machine at a temperature of 20 ± 2° C. Uniaxial tensile tests were carried out on specimens of cross sectional 5 mm x 3 mm and gauge length 50 mm at an applied strain rate of 5 x 10^{-4} sec^{-1}. Uniaxial compression tests were carried out as in [4], by placing a strip of cross section 3 mm x 3 mm at right angles across the 3 mm wide anvils of a Ford plane strain compression apparatus [6], so that the deforming region is approximately a cube. Ford plane strain compression tests were carried out with anvil widths of 3 and 6 mm on 30 mm lengths of sheet. Plane strain compression tests were also carried out with a slot and anvil apparatus. Fig. 7 shows the initial apparatus in which the slot is 3 mm wide, and the 19 mm long anvil is shorter than the POM specimen. The effect of the ends of the anvil in indenting the top face of the specimen is to prevent any shear of the specimen in the R′T′ plane, even though the polished steel surfaces were sprayed with a fluorocarbon spray. Subsequently further tests were made with an instrumented slot and anvil apparatus

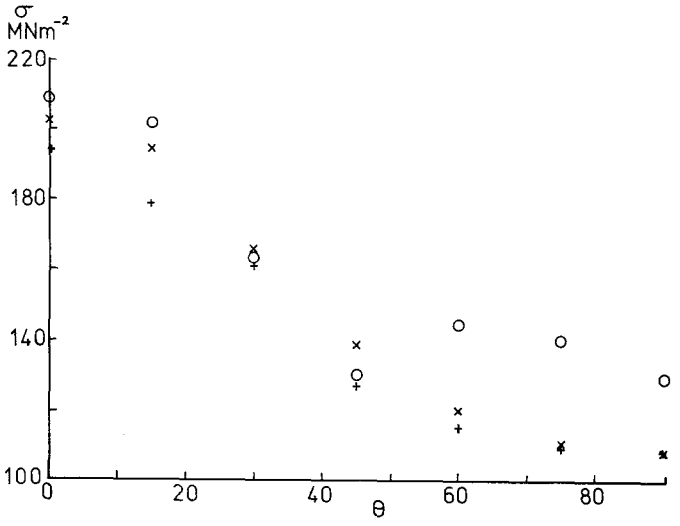

Figure 8 Measured plane strain compression yield stresses in the R'N plane for POM rolled to $\epsilon_R = 0.69$. Width to height to deformed zone = 1 for +, 2 for × and 7 for ○.

[10] that was capable of measuring the constraining stress perpendicular to the slot wall. In this case the slot was narrower (2.5 mm) and the specimen shorter (10 mm) than the anvil, and the anvil was free to move parallel to the length of the slot, the result being that the specimen is free to develop a shear $e_{T'R'}$. At one stage, a set of roller bearings was imposed between the Instron crosshead and the anvil to lessen any constraint on the anvil movement, but this had very little effect on the results. The strain rate in all the compression tests was approximately 10^{-3} sec^{-1}.

3.2. Results of yield stress tests

A different definition of the yield point was necessary for the tensile tests, than for the compression tests. For the former, all the specimens developed a neck, the neck initiating at a maximum in the load–deflection curve, at a strain of approximately 0.05. The tensile yield stress was taken as the true stress at the load maximum, since there was no evidence of permanent plastic deformation of samples unloaded before reaching this point. In nearly all the compression tests, there was a decrease in the positive slope of the load–deflection curves at a point which concided with the onset of plastic deformation. The yield point was defined by the intersection of two tangent lines fitted to straight portions of the load–deflection curve [11].

Although in the plane strain compression experiments the polished metal surfaces in contact with the POM were lubricated with a fluorocarbon spray, there was a possibility that the measured yield stresses were elevated by friction at the polymer-metal surface. Therefore a cross check was made, using three pieces of equipment, of the yield stress anisotropy under plane strain deformation in the R'N plane of POM rolled to $\epsilon_R = 0.69$. In the plane of deformation the width to height ratio of the deformed zone was varied from 1 to 2 using Ford anvils of different widths, and to 7 using the slot apparatus. A slip line field analysis [12] shows that, for anvil widths that are integral multiples of the sheet thickness, the slip lines are straight and the consequently indentation pressure to cause yielding is independent of the anvil width. Fig. 8 shows that the results agree reasonably well,

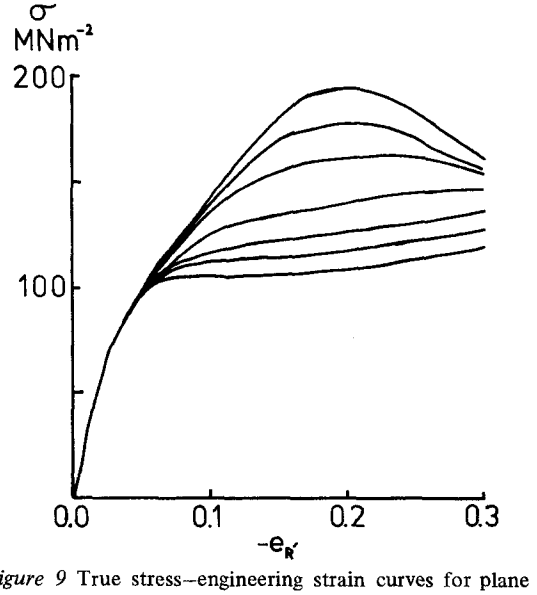

Figure 9 True stress–engineering strain curves for plane strain compression in the R'N plane of POM rolled to $\epsilon_R = 0.69$. Width to height of deformed zone = 1. Values of θ from 0° to 90° in 15° intervals, the uppermost curve being for $\theta = 0$, and the lowest for $\theta = 90°$.

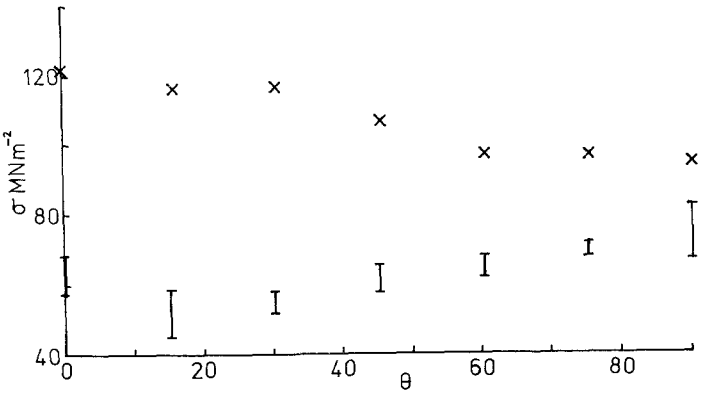

Figure 10 Angular variation of applied compressive stress x, and constraining stress in N direction I, for plane strain compression in the RT plane of POM rapidly rolled to $\epsilon_R = 0.87$.

with the results from the slot apparatus being at most 20% above those from the Ford apparatus. At a width to height ratio of 1 another effect manifests itself in the Ford test, that of localized shear bands running in the directions of maximum shear stress from the edges of the compression anvils. Fig. 9 shows the stress–displacement curves for the range of θ values used. For θ values $\leqslant 30°$ the stress–strain curve goes through a maximum, and can no longer be approximated by two straight lines. For this angular range cracks developed in the POM, starting at the edges of the compression anvils, and propagating in the direction of the localized shear bands. This cracking only occurred after the maximum in the stress strain curve, and must be the reason for the observed decrease in stress. For this angular range the maximum stress observed was taken as the yield stress, which Fig. 8 shows is a reasonable assumption.

Fig. 10 shows the results of measuring both the applied stress in the T′ direction and the constraining stress in the N direction for the instrumented slot tests. The rapidly rolled POM sheet used in this test had a lower yield stress anisotropy than the other materials used, and pole figure measurements showed that it had a weaker texture. It is clear that the ratio of the two stresses is not 2:1 as would be the case for a material obeying the Von Mises yield criterion.

3.3. Use of experimental data to determine the parameters of the POM deformation model

The parameters of the deformation model are

(1) CHAIN: the critical resolved shear stress for chain slip in an undeformed crystal.

(2) PRISM: the critical resolved shear stress for prism slip.

(3) SHC: the shear hardening coefficient for chain slip.

(4) M: the minimum reverse yield stress for chain slip divided by CHAIN.

It was possible to estimate the average value of CHAIN and PRISM by calculating the yield stresses of isotropic POM as a function of the angle θ in the sheet. The initial set of 187 Euler angles from the texture prediction program [5], which was known to give isotropic pole figures, was used for these calculations. The results given in Table I, are the average values for $90° \geqslant \theta \geqslant 0°$, with the range of values given in brackets.

The isotropy of the predicted yield stresses, and the agreement to within 3 MN m^{-2} of the Ford and slot test predictions, shows that there is no inherent anisotropy producing faults in the programs. Without making a pressure correction the ratio of the predicted plane strain to uniaxial yield stresses is 1.18, which is close to the value $2/\sqrt{3}$ that a material obeying the Von Mises yield criterion would have. It can be seen from Table I that it is necessary to include a pressure dependent term in the yield criterion of POM to attempt to

TABLE I Yield stresses of isotropic POM at 20° C (MN m^{-2}). Model parameters CHAIN = PRISM = 35 MN m^{-2}

Test	Predicted values		Experiment
	no pressure dependence	with pressure dependence	
Ford P.S. compression	98.0 (0.3)	108.6 (0.5)	117 (2)
Slot P.S. compression	95.6 (0.3)	105.7 (0.5)	130
Uniaxial compression	81.9 (0.3)	86.6 (0.3)	85 (2)
Uniaxial tension	81.9 (0.3)	77.2 (0.3)	66

match the experimental yield stresses. The experimental values of plane strain compression yield stresses will be overestimates since no correction has been made for frictional forces. Consequently a reasonable average value for CHAIN and PRISM is 35 MN m^{-2}.

In the earlier comparison of the experimental and predicted stress strain curves for the plane strain compression of initially isotropic POM (Fig. 3) a value for SHC of 0.4 was obtained. However this value depends on the ratio of PRISM:CHAIN used, a ratio of 2.5:1 being used there. As we wish to use the CHAIN:PRISM ratio as a disposable constant, the value of SHC may differ somewhat from 0.4. The magnitude of SHC will also depend on the accumulated shear strains in each crystal. This latter quantity is in doubt since the predicted textures at $\epsilon_R = 0.36$ (when the accumulated shear strain was 1.2) match the experimental textures at $\epsilon_R = 0.79$, and the predicted texture at $\epsilon_R = 0.69$ (accumulated shear strain 2.2) match the experimental textures at $\epsilon_R = 1.20$. The real accumulated shear strains may be larger if the rotation constraints are wrong; alternatively they may be approximately correct if the amorphous phase contributes significantly to the total strain.

A range of values of CHAIN/PRISM, SHC and M were used in the search for the most realistic predictions. As space limitations preclude showing a range of predicted results, the main effects of these parameters are briefly summarized below. First the yield stress tests can be classified as being "hard", "neutral" or "soft" according to whether the majority of crystals shear further on the same slip system as in prior rolling deformation, shear on other slip systems, or reverse the direction of shear on the same slip systems. The yield stress for a "hard" test such as the Ford or slot tests for $\theta = 0°$, is strongly dependent on the value of SHC. For "neutral" tests such as the Ford or tensile test at $\theta = 90°$, the ratio of PRISM:CHAIN is the most important parameter in determining the yield stress. For "soft" tests such as uniaxial compression at $\theta = 0°$, M is the most important parameter.

3.4. Comparison of predictions with experimental results

In Figs. 11–14 the experimental yield stresses are shown for tensile, compressive, Ford and slot tests respectively, for POM rolled to true strains ϵ_R = 0.69 and 1.20. (The latter value represents the limit of room temperature rolling before cracking occurs from the edges of the sheet). Predictions of the yield stress anisotropy are also made, using the textures displayed on the bottom rows of Figs. 4

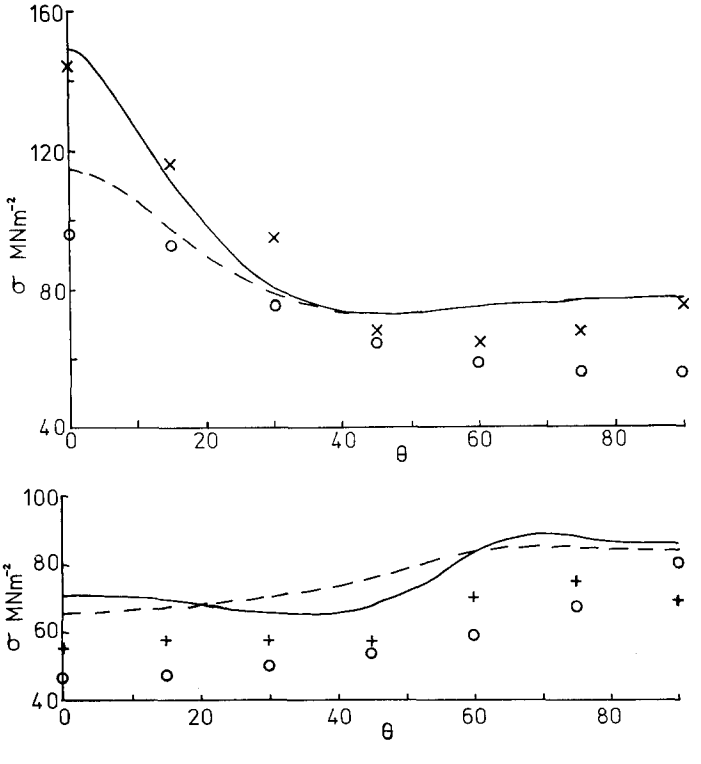

Figure 11 Angular variation of the uniaxial tensile yield stress in the plane of the sheet. Experiment results; $\epsilon_R = 0.69$ ○ and $\epsilon_R = 1.20$ ×. – – – – and ——— are the predictions for $\epsilon_R = 0.69$ and 1.20, using the textures shown on the bottom rows of Figs. 4 and 5 respectively, for CHAIN = PRISM = 35 MN m^{-2}, SHC = 0.4 and M = 0.5.

Figure 12 As in Fig. 11 but for the uniaxial compressive yield stress.

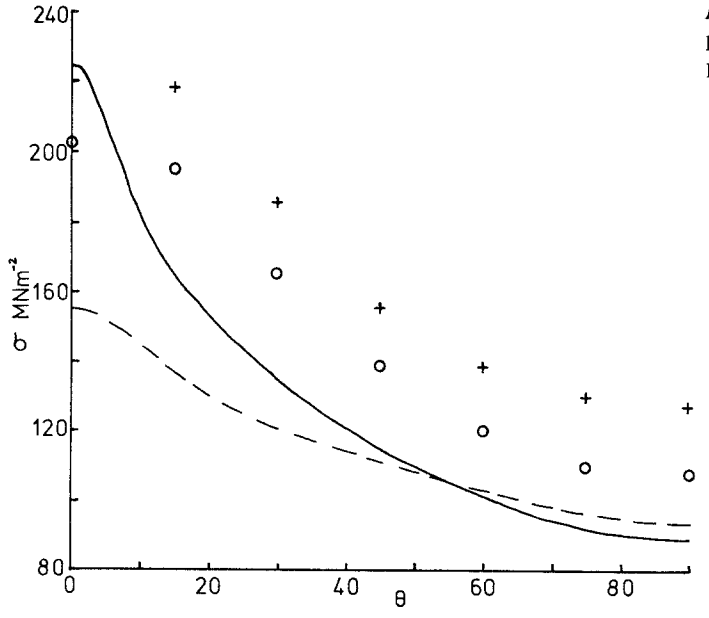

Figure 13 As in Fig. 11 but for the Ford plane strain compression test in the R'N plane.

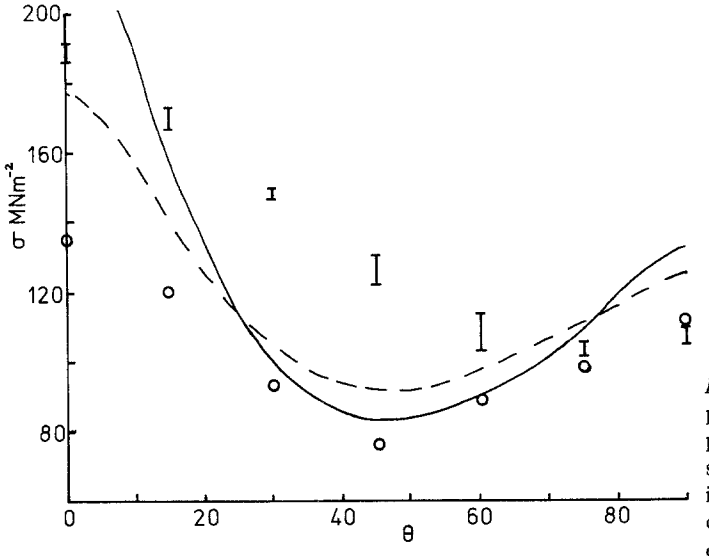

Figure 14 As in Fig. 11 but for the slot plane strain compression test in the RT plane. I is the range of experimental yield stresses for $\epsilon_R = 0.69$ when no shear strain is permitted. ○ is the stress to cause a strain of 0.1 when shear strains are permitted, for $\epsilon_R = 0.87$.

and 5, for the parameters CHAIN = PRISM = 35 MN m^{-2}, SHC = 0.4 and M = 0.5. Taking the results in turn, the following comments can be made.

The tensile yield stress predictions (Fig. 11) are correct to within ± 15 MN m^{-2}, and the overall agreement in shape is good. The relative increase from $\epsilon_R = 0.69$ to 1.20 is correctly predicted for $\theta < 45°$, but not at larger θ values; this suggests that the prism slip system may be hardened by prior deformation.

The uniaxial compression yield stress predictions (Fig. 12) are between 10 and 20 MN m^{-2} too high, but the correspondence of shape is good, and the relatively small change in yield stress due to further rolling is predicted well. The Ford plane strain compression yield stress predictions (Fig. 13) are between 15 and 40 MN m^{-2} too low, but otherwise the shape, and the increase due to further rolling are predicted reasonably well. The yield stress predictions may be low because the model assumes that shear strain can develop at

will, but the experimental apparatus does not allow this. The failure to predict an increase in yield stress at $\theta = 90^\circ$ with further rolling may again be due to a possible hardening of the prism slip system.

The model predicts that the slot plane strain compression yield stresses should have a minimum value at $\theta = 45^\circ$ (Fig. 14). This is presumably a result of assuming that the polycrystalline aggregate is free to develop a shear strain in the R′T′ plane. In the first set of experiments, when such a shear strain was not allowed to develop, the yield stress shows a monotonic decrease from $\theta = 0$ to $\theta = 90^\circ$ (data is not shown for $\epsilon_R = 1.20$ because the double tangent method of determining the yield point could not be applied for $\theta < 30^\circ$). In the second set of experiments, testing rapidly rolled POM in the instrumented slot device, Fig. 10 has already shown that the same monotonic decrease in yield stress occurs, even if the specimen is free to shear. However the yield strain, defined by the double tangent yield point construction, varied markedly with θ, as did the rate of "work" hardening after yield. To overcome this variation, Fig. 14 also shows the stress to cause a total (elastic and plastic) strain of 0.10 for the second experiment. This data does show a minimum stress at $\theta = 45^\circ$, and the stress values are fairly close to the predictions. However the stresses are always below the yield stress defined by the double tangent construction, so it could be argued that POM shows a minimum at $\theta = 45^\circ$ only in the elastic modulus, and not in the yield stress.

Considering Figs. 11–14 together, it can be seen that rolling from $\epsilon_R = 0.69$ to $\epsilon_R = 1.20$ increases the yield stress significantly only in "hard" direction tests, in which the stronger texture and increased shear hardening of chain slip combine to increase the yield stress. The predicted yield stresses in these "hard" direction tests are sensitive to the precise texture used for prediction. Since the actual texture cannot be measured with great precision this means that a comparison of actual and predicted yield stresses in "hard" direction tests is not a good way of determining the model parameters. Conversely in "neutral" or "soft" direction tests, the predicted yield stresses are not so critically dependent on the assumed texture, so comparisons with experimental values provide a better way of determining model parameters.

TABLE II Critical resolved shear stresses (MN m^{-2}) for deformation processes in semicrystalline polymers

Polymer	Volume fraction crystallinity	Slip direction	
		parallel to *c* axis	perpendicular to *c* axis
Polyethylene (13)	0.77	15	–
Polypropylene (4)	0.55*	25	25
POM	0.74	35	35

* prior to orientation

4. Discussion

The model for the yield anisotropy of POM has two main advantages over previous models. Firstly it has been possible to estimate the stresses at which certain deformation mechanisms operate, including such refinements as shear hardening and a Bauschinger effect. Table II compares our estimates of the critical resolved shear stresses of POM with estimates for other polymers.

The values in Table II make no allowance for the amorphous content of the polymers. The values for polyethylene and polypropylene are only approximate, as the slip plane is not specified, and the values were calculated assuming a material of perfect *c* axis orientation. However all the results are of the same order of magnitude.

The second achievement is to have a guide, even though imperfect, to how certain deformation processes change the texture, and hence the yield anisotropy of POM. (Drawing under a tensile stress must be excluded since other deformation processes such as microvoiding occur). We have used four parameters to give the best match between predicted and experimental yield stress values, but the advantage over the use of yield criteria such as that of Hill is that our parameters are independent of the texture of the polymer, and they are amenable to experimental confirmation. It is worth noting that two of the parameters, the mean of CHAIN and PRISM, and the shear hardening coefficient SHC, have been obtained from other yielding measurements on isotropic POM. It is hoped that further experiments on highly oriented forms of POM will provide independent estimates of the model parameters.

The hypothesis of how a Bauschinger effect operates in each *crystal* is unlikely to be correct in detail, but it is preferable to the hypothesis of a macroscopic Bauschinger effect [2]. The latter only provides an internal stress in one direction, R,

and provides no clue as to how such a uniform internal stress could arise (the stress required is too large to be due to the deformation of any long range rubber-like network that exists in the semi-crystalline polymer). In contrast the internal stresses in each *crystal* are locked into the polycrystalline aggregate by the surrounding *crystals* of differing orientation, and cannot be released until further plastic deformation of the polymer occurs.

There are a number of weaknesses in the model for the plastic deformation of POM that exist because of our ignorance of details of deformation processes, or because of the simplicity of the model. One obvious weakness is that textural development does not occur as fast as predicted on rolling POM, and the rotations of crystal axes that occur when chain slip occurs are not in the precise direction predicted. This fault arises because of our ignorance of the real constraints that cause *crystals* to rotate when they plastically deform. As deformation proceeds the *crystals* will develop a non-equiaxed shape, that will depend on the position of the *crystal* in the spherulite. The *crystals* will be surrounded by others of similar shapes and orientation. We have observed that when two dimensional POM spherulites are deformed on a polyethylene terephthalate film substrate that different deformation mechanisms occur in different sectors of the spherulite (Fig. 15). It is hardly surprising that our neglect of the spherulitic microstructure and assumption that the same constraints for crystal axis rotation exist regardless of the anisotropy of the surrounding material, causes the predicted texture to be incorrect in detail. The decision in Section 2.1, to suppress the reorientation by prism slip of crystals that have undergone extensive chain slip, is understandable when it is realized that these crystals are surrounded by others also having their c axes closely oriented towards the rolling direction. It is unlikely that any major reorientation of crystal axes could occur in such an anisotropic environment.

A second failing is that too much 'transverse' $\{1\,\bar{2}\,1\,0\}\langle 1\,0\,\bar{1}\,0\rangle$ texture is predicted to develop on rolling if the ratio of critical resolved shear stresses used is CHAIN:PRISM = 1:1 (this ratio gives the best yield anisotropy predictions from the observed texture). A possible explanation is that a process of lamellar breakdown and reformation of microfibrils [14] occurs in *crystals*

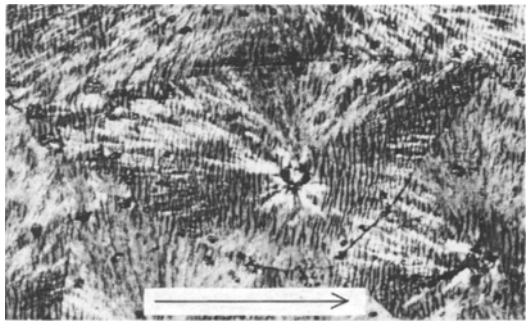

Figure 15 Micrograph of a two dimensional POM spherulite that has been extended by 10% on a 'Mylar' substrate. The arrow shows the direction of extension.

with a transverse orientation. This would reduce the transverse component of texture while increasing the amount of c-axis fibre texture. Transverse orientations occur in the spherulite sector that is roughly parallel to the rolling direction. Fig. 15 shows that microcracking occurs in such sectors when spherulites are extended on a substrate, and such microcracking would be a useful precursor to the lamellar breakdown deformation mechanism.

We have assumed that there is a nearly uniform state of stress in the deforming polycrystalline aggregate, and consequently we have neglected the displacement mismatch that will occur at the *crystal* boundaries. This can be excused on the grounds that neighbouring *crystals* in a spherulite will have fairly similar orientations, and that the amorphous phase may take up some of the displacement mismatch. Predictions of the elastic anisotropy of semi-crystalline polymers [15] have also used the uniform stress assumption. On the other hand recent predictions of the yield stress anisotropy of metals [16, 17] have used a uniform strain assumption for the polycrystalline aggregate. In the case of metals each grain is likely to be surrounded by others of initially random orientation, and there is no amorphous phase to absorb any displacement mismatch between grains.

The yield behaviour of anisotropic forms of other semi-crystalline polymers, such as high density polyethylene, polypropylene and polyethylene-terephthalate, is roughly similar to that described here, although data is often restricted to one or two types of yield test [4, 13, 15]. This suggests that the theoretical approach presented here could be applied with advantage to these other polymers. However there are difficulties;

oriented polypropylene often contains microvoids which could subsequently provide deformation modes that are difficult to attribute stress levels to; polyethylene not only has a less symmetric unit cell than POM, but it can also deform by twinning and by a martensitic phase transformation.

Finally we will consider the technological relevance of this research. The original reason for the measurement of the plane strain yield stresses of POM was to be able to analyse the deep drawing performance [18]. It was found that uniaxially rolled POM had an undesirable degree of anisotropy in the plane of the sheet, whereas biaxially rolled POM did not have this disadvantage. Even so the desirable increase in the in-plane yield stress was accompanied by an undesirable increase in the rate of strain hardening, so the limiting draw ratio for the fabrication of cups from circular blanks was little increased. This can now be explained by saying that the desirable texture developed in biaxially rolled POM could not be achieved without a simultaneous accumulation of shear strain in the *crystals*. It is impossible to remove this undesirable shear strain accumulation by the partial recrystallization that occurs below the melting point of POM; and if POM is melted then both the texture and the accumulated shear strain are lost. The phenomenon of work hardening as such does not exist in POM; mechanical deformation does not increase all the yield stresses equally. It is apparent from this study that one of the major causes of the increase of the yield stress of POM is the shear hardening of the chain slip mechanism. This mechanism causes the rolled POM to have a large Bauschinger effect, so that the yield stress in certain compression tests is the same as for isotropic POM or even less. Thus it is clear that the possibilities of improving the overall balance of yield stresses of POM by mechanical deformation are slight.

Acknowledgements

N.D.C. and M.J.M. would like to thank the Science Research Council for support in the form of research studentships.

References

1. R. HILL, "The mathematical theory of plasticity", (Oxford University Press, Oxford, 1950) p. 317;
2. N. BROWN, R. A. DUCKETT and I. M. WARD, *Phil. Mag.* **18** (1968) 483.
3. A. KELLER and J. G. RIDER, *J. Mater. Sci.* **1** (1966) 389.
4. D. SHINOZAKI and G. W. GROVES, *ibid* **8** (1973) 71.
5. M. J. MILES and N. J. MILLS, *ibid* **10** (1975) 2092.
6. J. G. WILLIAMS and H. FORD, *J. Mech. Eng. Sci.* **6** (1964) 405.
7. G. Y. CHIN and W. L. MAMMEL, *Trans. Metal. Soc. AIME* **239** (1967) 1400.
8. D. SARDAR, S. V. RADCLIFFE and E. BAER, *Poly. Eng. Sci.* **8** (1968) 290.
9. A. W. CHRISTIANSEN, E. BAER and S. V. RADCLIFFE, *Phil. Mag.* **24** (1971) 451.
10. C. H. LLOYD, C. N. REID, B. METCALFE and E. AMINI, *Metal Science* **9** (1975) 415.
11. I. M. WARD, *J. Mater. Sci.* **6** (1971) 1397.
12. G. W. ROWE, "An Introduction to the principles of metalworking" (Arnold, London, 1965) p. 79.
13. R. J. YOUNG, P. B. BOWDEN, J. M. RITCHIE and J. G. RIDER, *J. Mater. Sci.* **8** (1973) 23.
14. A. PETERLIN, in "Polymeric Materials" (American Society of Metals, Metals Park, Ohio, 1975).
15. D. W. HADLEY and I. M. WARD, in "Structure and properties of oriented polymers" edited by I. M. Ward. (Applied Science Publishers, London, 1975) Chapter 8.
16. H. J. BUNGE and W. T. ROBERTS, *J. Appl. Cryst.* **2** (1969) 116.
17. J. S. KALLEND and G. J. DAVIES, *J. Inst. Metals* **98** (1970) 257.
18. M. J. MILES and N. J. MILLS, *Poly. Eng. Sci.* **17** (1977) 101.

Received 18 October and accepted 16 December 1976.